

---

**Original Article****Bone marrow-derived stromal cells can express neuronal markers by DHA/GPR40 signaling**

Desislav B. Kaplamadzhiev<sup>1</sup>, Hiroko Hisha<sup>2</sup>, Yasushi Adachi<sup>2</sup>, Susumu Ikehara<sup>2</sup>, Anton B. Tonchev<sup>3</sup>, Nadezhda B. Boneva<sup>1</sup>, Ilia V. Pyko<sup>1</sup>, Mitsuru Kikuchi<sup>4</sup>, Masa-aki Nakaya<sup>5</sup>, Tomohiko Wakayama<sup>5</sup>, Shoichi Iseki<sup>5</sup>, Tetsumori Yamashima<sup>1,\*</sup>

<sup>1</sup> Department of Restorative Neurosurgery, Kanazawa University Graduate School of Medical Science, Kanazawa, Japan;

<sup>2</sup> First Department of Pathology, Kansai Medical University, Osaka, Japan;

<sup>3</sup> Laboratory of Cell Biology, Medical University-Varna, Varna, Bulgaria;

<sup>4</sup> Departments of Psychiatry and Neurobiology, Kanazawa University Graduate School of Medical Science, Kanazawa, Japan;

<sup>5</sup> Departments of Histology and Embryology, Kanazawa University Graduate School of Medical Science, Kanazawa, Japan.

---

**Summary**

The exact origin of neural stem cells in the adult neurogenesis niche remains unknown. Our previous studies, however, indicated an implication of both bone marrow cells as potential progenitors of hippocampal newborn neurons and polyunsaturated fatty acids as ligands of G protein-coupled receptor 40 (GPR40) signaling. Here, we aimed at studying whether bone marrow-derived stromal cells (BMSC) treated by docosahexaenoic acid (DHA) can express neuronal markers *in vitro*. We focused on implication of DHA/GPR40 signaling for the expression of neuronal markers in clonally-expanded BMSC from young macaque monkeys. Cell cycle analysis revealed that the DHA plus bFGF treatment induced a decrease of BMSC proliferation and increased the cells in the G<sub>0</sub> resting phase. The transitions from nestin-positive progenitors *via* immature neuronal ( $\beta$  III-tubulin-positive) to mature neuronal (NF-M and Map2-positive) phenotypes were examined using RT-PCR, Western blot and immunocytochemistry. We detected a significant increase of GPR40 mRNA and protein expression after bFGF induction, being compared with the untreated BMSC. Addition of DHA, a representative GPR40 ligand, led to a significant down-regulation of GPR40, *i.e.*, G protein-coupled receptor-specific internalization, with a subsequent upregulation of neuronal markers such as  $\beta$  III-tubulin, NF-M and Map2. These data altogether suggest that adult primate BMSC can express neuronal markers with the aid of DHA/GPR40 signaling.

**Keywords:** Bone marrow-derived stromal cells (BMSC), docosahexaenoic acid (DHA), basic fibroblast growth factor (bFGF), G protein-coupled receptor 40 (GPR40), monkey

---

**1. Introduction**

The G protein-coupled receptor 40 (GPR40) gene was first identified in the pancreas and brain of humans in 2003 (1,2). Subsequently, polyunsaturated fatty acids (PUFA) such as docosahexaenoic acid (DHA), eicosapentaenoic acid (EPA) and arachidonic acid were

found to be endogenous ligands of GPR40 (1-3). The implications of this receptor for the insulin secretion in the pancreas have been extensively studied. However, except for ours (4-6), there are no reports studying the role of GPR40 in the brain, even though this receptor is widely distributed in the central nervous system (CNS) (1). Recently, Ma *et al.* found upregulation of the GPR40 expression in the primate neural stem cell niche after transient global ischemia (4). Furthermore, using rat neural stem cells devoid of GPR40, they confirmed that the DHA-induced neuronal differentiation of these cells occur after transfection of GPR40 gene (6). These findings reinforced a putative involvement of PUFA/GPR40 signaling in the neurogenic niche of the adult

---

\*Address correspondence to:

Dr. Tetsumori Yamashima, Department of Restorative Neurosurgery, Kanazawa University Graduate School of Medical Science, Takara-machi 13-1, Kanazawa 920-8641, Japan.  
e-mail: yamashim@med.kanazawa-u.ac.jp

brain (5).

Biological effects of PUFA, particularly DHA, are thought to include incorporation into cell membrane phospholipids thus preserving membrane fluidity, its modulation of DNA transcription, or its effect on the synthesis of ATP in the mitochondria. However, it is also probable that DHA may serve as a secreted ligand that can bind with the GPR40 receptor and elicit intracellular signaling for the regulation of adult neurogenesis (5). There are several lines of evidence supporting this possibility. First, GPR40 couples mainly with the G protein  $\alpha$ -subunit of the Gq family resulting in elevation of intracellular  $\text{Ca}^{2+}$  and stimulation of protein kinase C (PKC) activity (1,2,6). Second, after transfection of GPR40 into PC12 cells, they show a transient  $\text{Ca}^{2+}$  mobilization in response to arachidonic acid (5) which is functionally similar to DHA, regarding its ability to induce neuronal differentiation (7). Third, accumulating data indicate involvement of DHA in the differentiation of neural stem/progenitor cells (NSC) (6,8-10), embryonic stem (ES) cells (11), and bone marrow-derived mesenchymal stem cells (BM-MSC) (7). Moreover, DHA contributes to survival and neurite outgrowth in the primary culture of cortical neurons (12), hippocampal neurons (9), and ES-derived neuronal cells (11). Finally, data from clinical studies demonstrate improvement of visual acuity (13) and cognitive ability (14) in infants who were given a formula supplemented with DHA plus arachidonic acid or DHA alone. At the same time, a deficiency of DHA results in a poor performance on cognitive and behavioral tests, while the supplementation with DHA recovers learning ability and memory-related performance in experimental animals (15) as well as in human patients with memory impairment (5).

The adult hippocampus of mammals, including primates, retains regeneration capability from neural stem cells generating granule neurons in the dentate gyrus. The exact origin of these progenitors has been a subject of extensive research, however, there is no worldwide consensus about this. It has been previously suggested that the vascular adventitia is a potential precursor cell source in the neurogenic niche of adult monkey hippocampus (16). This suggestion has been subsequently supported by the discovery of cells that were enriched in markers of neural tissue-committed stem cells residing in bone marrow and mobilized "on demand" into the peripheral blood following stroke (17). It is now accepted that such stem cells and the above-mentioned perivascular neural progenitors (16) may share a common origin, being regarded as *in situ* counterparts of bone marrow stroma (18). Notably, endogenous hippocampal progenitors as well as bone marrow stromal cells express GPR40 (1,4,19). The changes in the brain PUFA composition of rats with cerebral ischemia following transplantation of BM-MSC (20) further support such possibility that the

postischemic enhancement of adult neurogenesis might be PUFA-dependent presumably *via* GPR40 activation. Based on these data, we designed an experimental paradigm, in which the expression of GPR40 and a set of neuronal markers such as nestin,  $\beta$  III-tubulin, NF-M, and Map2 were examined in clonally-expanded BMSC. BMSC were induced to express neuronal phenotype by bFGF as previously described (21), and the effect of DHA, a representative GPR40 receptor ligand (1-3) was evaluated.

## 2. Materials and Methods

### 2.1. Harvest of monkey bone marrow cells (BMC)

Animal experiments were performed at the Institute for Experimental Animals, Kanazawa University Advanced Science Research Center. Surgical procedures and postoperative care of animals were in accordance with its guidelines and those of the National Institutes of Health for Care and Use of Primates. Three infant monkeys (*Macaca fuscata*) weighing 2-3 kg supplied by National Bioresource Project (Okazaki, Japan), were used for the BMC harvest. The contamination of the collected BMC with peripheral blood was prevented (22). Under general anesthesia with 1-1.5% fluothane mixed with 33%  $\text{O}_2$  and 67%  $\text{N}_2\text{O}$ , a skin incision of 10 cm was made and the femoral bone surface was disclosed. Two aspiration needles (Angiotech, DBMNI 1601 - 16G) were inserted into the bone marrow cavity at proximal and distal span. The BMC samples were collected in a sterile 50 mL Falcon tube containing 30 mL Dulbecco's phosphate buffered saline (DPBS) and 2500E heparin sodium salt (Sigma-Aldrich, H3149) by perfusion.

### 2.2. Experimental groups

Clonally-derived BMSC were cultured in the neurobasal media with N-2 supplement (R&D Systems, AR003) without serum. The specific reagents of interest were added to the medium as adopted from previous experiments of *in vitro* differentiation of NSC or neuronal induction of multipotent stromal cells from bone marrow (21,23-26). Experimental groups were as follows: neuronal phenotype induction with bFGF, DHA alone without bFGF, and DHA plus bFGF.

### 2.3. Expansion of BMSC

Single-cell suspension from fresh BMC (30 mL) was layered over density gradient media (Axis-Shield, Lymphoprep, 1114544) and centrifuged for 30 min,  $150 \times 10$  rpm at  $20^\circ\text{C}$ . Mononuclear fraction of whole BMC samples was collected at the interface and re-suspended at  $1 \times 10^4/\text{cm}^2$  in 5 mL growth media (GM) in Cell Culture Flask,  $25 \text{ cm}^2$  (BD Biosciences Labware, BD BioCoat, 354532). GM contained: minimum essential

medium alpha ( $\alpha$ -MEM) with GlutaMAX (Invitrogen, GIBCO, 32571036), 10-15% fetal bovine serum (FBS) MSC-Qualified (Invitrogen, GIBCO, 12662029), and 1% antibiotic-antimycotic (Invitrogen, GIBCO, 15240062). Adherent cells were kept and after 50-60% confluence, BMSC were transferred and further expanded from single-cell colonies derived by serial dilution in 48 well plates (Corning, Cell Wells, 258301). Each well containing less than 10 adherent cells after 8 hours of incubation was further expanded. Clonal expansion of  $0.5-1 \times 10^3/\text{cm}^2$  BMSC from single-cell derived colonies was cultured in 5 mL expansion media (EM). The medium contained the same reagents described for the GM except that the FBS concentration was lowered to 3%. For non-clonal expansion  $1 \times 10^4/\text{cm}^2$  adherent BMSC were incubated in 5 mL GM. Cell viability was evaluated by trypan blue (0.5%, w/v in DPBS) exclusion. At least 90% viability was confirmed prior to each sub-culturing. Cumulative population doubling (CPD) was calculated by counting viable cells with a hemocytometer chamber.

#### 2.4. Differentiation of BMSC to adipocytes, osteoblasts and chondrocytes

To induce adipogenic differentiation, clonally-expanded BMSC were incubated in 3 cycles with adipogenic induction/maintenance medium (Cambrex Bio Science, PT-3004) following the manufacturer's instructions. Osteogenic differentiation was induced from subconfluent clonally-expanded monkey BMSC cultured in an osteogenesis induction medium (Cambrex Bio Science, PT-3003) for 5 weeks in flasks until morphological changes could be seen. Chondrogenic differentiation was performed according to the standard protocol in chondrogenic medium (Cambrex Bio Science, PT-3003) for 5 weeks.

#### 2.5. FACS analyses of BMSC

Clonally-derived populations of BMSC from expansion adherent culture were stained with fluorescein isothiocyanate (FITC)- or phycoerythrin (PE)-conjugated monoclonal antibodies (mAbs) against non-human primate CD3, CD4, CD8, CD14, CD29, CD31, CD34, and CD45 (BD Biosciences, San Jose, CA); against human CD90 (Biotrend, Germany), CD73 (BD Pharmingen, CA, USA), and CD105 (Serotec, UK). The stained cells were analyzed using a FACScan (Becton Dickinson, Mountain View, CA).

#### 2.6. Induction of neuronal phenotype in BMSC

$0.5-1 \times 10^5$  clonally-expanded BMSC were cultured in 5 mL neuronal medium in 25  $\text{cm}^2$  flasks (BD Biosciences Labware, BD BioCoat, 354532). The medium contained: neurobasal media (Invitrogen,

GIBCO, 21103049), L-alanyl-L-glutamine a dipeptide substitute for L-glutamine (Invitrogen, GIBCO, GLUTAMAX, 35050061), N-2 Plus media supplement (R&D Systems, AR003), 1% antibiotic-antimycotic (Invitrogen, GIBCO, 15240062). Neuronal commitment with bFGF (Sigma-Aldrich, Fibroblast growth factor-basic from bovine pituitary, F5392) was adopted from previous works (21,26). DHA (Sigma-Aldrich, *cis*-4,7,10,13,16,19-docosahexaenoic acid, D2534) was continuously added to the culture medium for 14 days. bFGF was used in 10 ng/mL working concentration and DHA was used as bovine serum albumin (BSA) complexes with DHA at 10  $\mu\text{M}$  final concentration.

#### 2.7. Immunocytochemical analysis

Cells were grown in a Lab-Tek-Chamber Slide System (Nalge Nunc International, Permax, 177437) at the following seeding densities;  $0.5-1 \times 10^3/\text{cm}^2$  for clonal expansion and  $1 \times 10^5/\text{cm}^2$  for neuronal phenotype induction. These were then fixed and stained with IABs as follows: rabbit anti-GPR40 (1:100) (4,27), mouse anti-GPR40 (1:250, TransGenic Inc., Japan, Clone No. G16, KAL-KG116), mouse anti-nestin (1:200, Chemicon, Millipore, MAB5326), mouse anti-neuronal  $\beta$  III-tubulin (1:500, Covance, Clone Tuj1, MMS-435P), mouse anti-neurofilament medium chain, NF-M (1:1,000, Chemicon, Millipore, MAB5254), rabbit anti-Map2 (1:1,000, Chemicon, Millipore, AB5622). Secondary antibodies (IIAb) were applied for 2 h at 1:200 dilution, in green: anti-rabbit Alexa Fluor 488 (Invitrogen, A11034), anti-mouse Alexa Fluor 488 (Invitrogen, A11001) and in red: anti-rabbit Alexa Fluor 546 (Invitrogen, A11010), anti-mouse Alexa Fluor 546 (Invitrogen, A11018). Digital images were acquired using a confocal laser scanning microscope (LSM 510; Carl Zeiss, Tokyo, Japan) and LSM 510 software (version 3.2 SP2, Carl Zeiss, Germany). The number of positive cells of the whole visual field (magnification  $5\times$ ) was determined as a percentage of the total number of DAPI-labeled cell nuclei. In a representative experiment, a total of 300 cell nuclei positive for DAPI (100%) per 3-5 random visual fields were counted for any given expression marker.

#### 2.8. Western blotting

Protein extraction was done with RIPA buffer (Sigma-Aldrich, R0278) and Protease Inhibitor Cocktail (Sigma-Aldrich, P8340); for GPR40 experiment samples 0.1% Triton-X was also used. Total protein concentration in the supernatant was estimated by Bradford assay using sample preparation reagents (Bio-Rad, 500-0005, 500-0006) and spectrophotometer (GE Healthcare, GeneQuant pro RNA/DNA Calculator, 80-2114-98). For each experiment, 20  $\mu\text{g}$  total protein were added to a 20  $\mu\text{L}$  solution containing 1:1 (v/v)

sample in sample buffer (4× Tris-Cl/SDS, pH 6.8, 125 mM; 20% Glycerol; 4% SDS; DTT 0.2 M; ~0.01% bromophenol blue) and denatured at 100°C for 3 min. The electrophoresis was done in Laemmli's buffer system mini-gel (Bio Craft, BE-111) and transferred to PVDF membrane (ATTO, Japan, Clear Blot Membrane-p, AE-6667). IAb and dilutions were as follows: mouse anti-GPR40 (1:1,000, TransGenic Inc., Japan, Clone No. G16, KAL-KG116), rabbit anti-GPR40 (1:1,000) (4,27), mouse anti-*nestin* (1:1,000, Chemicon, Millipore, MAB5326), mouse anti- $\beta$  III-tubulin (1:500, Sigma-Aldrich, Clone SDL.3D10, T8660), rabbit anti-*Map2* (1:2,000, Chemicon, Millipore, AB5622) and mouse anti-NF-M (1:1,000, Chemicon, Millipore, MAB5254). A horseradish peroxidase-conjugated anti-rabbit or mouse IgG (1:10,000, Sigma-Aldrich) was used for visualization. A digital image of the signal from reacted proteins was acquired using an ECL Advanced Western Blot Detection Kit (GE Healthcare, PRN2135) and compact luminescent image analysis system (Fujifilm, LAS-4000mini) with LAS-4000mini Image Reader software v.2.0. Densitometric analysis was done using image processing software (NIH, ImageJ, 1.410).

### 2.9. Cell cycle analysis

BMSC were incubated with 10  $\mu$ M BrdU (Sigma-Aldrich, B9285) for 2 h and immunostained with rat anti-BrdU (1:100, Harlan SERA-LAB) and mouse anti-Ki-67 (1:100, DAKO, Clone MIB-1, M7240) primary antibodies. The same protocol described in the immunocytochemistry was used, except for the inclusion of a DNA denaturation step by incubation in 2 N HCl for 30 min at 37°C. The acid was neutralized by immersing the samples in borate buffer. Assessment of the proliferation capacity was performed with laser confocal microscope at 24 and 72 h after the induction of neuronal phenotype.

### 2.10. RNA extraction and RT-PCR analysis

Total RNA from the samples was isolated using TRI Reagent (Sigma-Aldrich, T9424). Gene specific primers for semiquantitative RT-PCR analysis was generated using the NCBI Primer-BLAST software

(<http://www.ncbi.nlm.nih.gov/tools/primer-blast/>) and NCBI Reference Sequences (whole genome assembly released by the Macaca mulatta Genome Sequencing Consortium as Mmul\_051212, February 2006, whole genome shotgun sequence, <http://www.hgsc.bcm.tmc.edu/projects/rmacaque/>) provided by NIH online resources. Reverse transcription was done with First-Strand Synthesis System for RT-PCR (Invitrogen, SuperScript III, 18080-051) from 1  $\mu$ g of total RNA with 50  $\mu$ M Oligo (dT)20. PCR reaction was carried out in thermal cycler (Applied Biosystems, Gene Amp 9700) with Platinum Taq DNA Polymerase High Fidelity (Invitrogen, 11304-011). Specific primers and conditions are shown in Table 1. Visualization of the corresponding band after electrophoresis in 2% Agarose gel (AMRESCO, Agarose HT, K449-500G) was done with ethidium bromide staining. A digital image was acquired using Luminescent Image Analysis System (Fujifilm, LAS-4000mini) with UV 2020 transilluminator set and image capture software, LAS-4000mini Image Reader v.2.0.

## 3. Results

### 3.1. Characterization of clonally-expanded BMSC

Clonally-expanded BMSC complied with the minimal criteria being suggested by the International Society for Cellular Therapy (28), and shared a certain similarity to mesenchymal stem cells in regards of expressed characteristic surface molecules. They sustained tri-lineage mesenchymal differentiation potential and extended self-renewal potential. Osteogenic induction was confirmed by von Kossa staining 4 weeks after the induction (Figure 1A). Adipogenic differentiation was confirmed by oil red O staining 5 weeks after the induction (Figure 1B). Furthermore, chondrogenic differentiation was confirmed by staining paraffin sections of the micromass with Alcian blue (Figure 1C).

Phenotype characterization of single cell-derived colonies of BMSC were obtained by flow cytometry. The cells were negative for lymphoid markers such as CD3, CD4, and CD8 (data not shown), an endothelial cell maker CD31, and hematopoietic cell markers CD14, CD34, and CD45 (Figure 1D). In contrast, BMSC were strongly positive for CD29 and CD90

**Table 1. List of specific primers and amplification conditions for RT-PCR**

| NCBI Accession | Aliases             | Sequence (5'-3')        |                        | Tm, Cycles | Size (bp) |
|----------------|---------------------|-------------------------|------------------------|------------|-----------|
|                |                     | Forward                 | Reverse                |            |           |
| XM_001094514.1 | GPR40 (FFAR1)       | GGCCTCACTGTGCCCTGTCT    | CAGGCTCCAGGCAGACG      | 56, 30     | 297       |
| XM_001116693.1 | Nestin              | GCAGGAGGAGTTGGGTCTCG    | TCCTCCCCCTCCTCCTCTTC   | 58, 30     | 276       |
| XR_011045.1    | $\beta$ III-Tubulin | ATCCGGACCCGATCATGAAC    | ACCATGTTGACGGCCAGCTT   | 58, 28     | 298       |
| XM_001106908.1 | NEF3 (NF-M)         | GCACATTTGCAGGAAGCATCAC  | GCTTCTGGCTCCTCCTCCTTTT | 58, 28     | 268       |
| XP_001105471   | GAPDH               | GCACATTTGCAGGAAGCATCAC  | GCTTCTGGCTCCTCCTCCTTTT | 60, 22     | 263       |
| XM_001109309.1 | Map2                | ACCGGAGAGGCAGAAATTTCCAC | AGCGCTTTTCTGGGCTCTTGGT | 58, 28     | 319       |

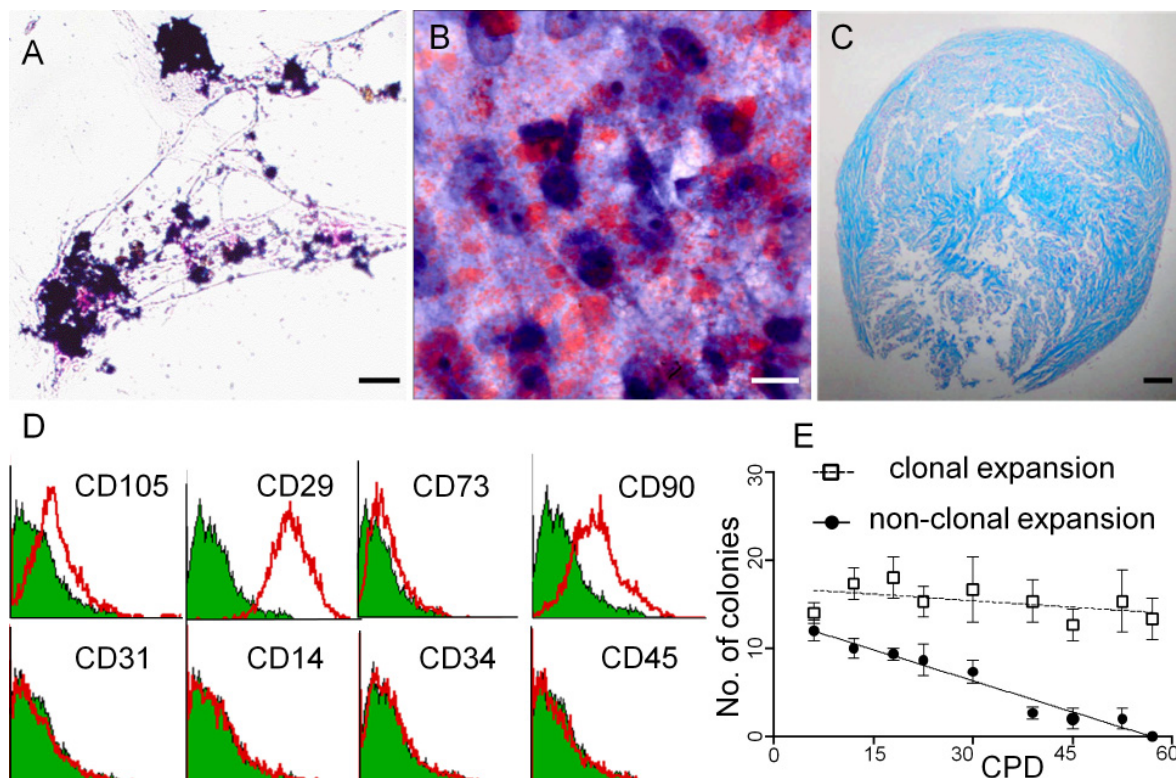


**Figure 1. Characterization of bone marrow-derived stromal cells (BMSC).** (A-C) Differentiation assay of clonally-expanded BMSC; A, osteogenic differentiation showing calcium deposition at 21 days of differentiation. von Kossa staining, Scale bar = 50  $\mu\text{m}$ ; B, adipogenic differentiation showing aggregates of lipid vacuoles at 35 days in adipogenic induction medium. Oil Red O staining, Scale bar = 20  $\mu\text{m}$ ; C, chondrogenic differentiation of the micromass positive for proteoglycan at 35 days in chondrogenic induction medium. Alcian blue staining, Scale bar = 100  $\mu\text{m}$ . (D) Surface molecules in BMSC – clonally-expanded BMSC stained with a panel of antibodies reacting with hematolymphoid markers and cell adhesion molecules analyzed by FACSscan. The green region indicates the cells stained with isotype-matched control. Representative staining patterns of three independent experiments. (E) BMSC obtained by adherence to plastic of mononuclear bone marrow cells and expanded from single cell-derived colonies denoted with open square (clonal expansion) were compared to non-clonal adherent BMSC in standard condition denoted with filled black circle (non-clonal expansion). Clonal expansion in the low serum condition selectively favored cells with potential for extended colony formation (number of the colonies on vertical axis) and self-renewal (number of cumulative population doublings – CPD on horizontal axis). These properties in non-clonally expanded BMSC on contrary decreased with the time in culture. ( $p < 0.0001$ ;  $\alpha = 0.05$ ,  $n = 3$ , error bars represent S.E.M.)

while weakly positive for CD73 and CD105. The negative staining for CD14 and CD31 indicated that the present clonally-expanded BMSC did not contain macrophages or endothelial cells. Single cell-derived colonies of monkey BMSC expanded in the low-serum at low-seeding density, showed a consistent colony formation and an extended subculture potential. On the contrary, non-clonal cultures maintained under standard condition with 10% serum at high seeding densities showed decreased ability to form colonies and limited subculture potential (Figure 1E).

### 3.2. Cell cycle analysis

We used a thymidine analogue BrdU incorporated into the cell during the S-phase and the expression level of Ki67 protein to track down the proliferation rate in the course of the experiment. Proliferation marker Ki67 ubiquitously labels all proliferating cells. By double immunostaining we assessed the number of cells, which upon exit from cell cycle halt the production of Ki67

and retain the BrdU trait, thus Ki67/BrdU<sup>+</sup> phenotype indicated differentiating or apoptotic cells. Analysis of cell proliferation 24 h after the BrdU inclusion in the cell culture media by BrdU/Ki67 labeling revealed no significant difference between the used protocols (data not shown). However, 72 h after neuronal induction and BrdU inclusion (Figure 2A), we found a significant decrease of the proliferation rate represented by the number of Ki67<sup>+</sup>/BrdU<sup>+</sup> cells in BMSC treated with bFGF and particularly in the group treated with DHA plus bFGF protocol, compared with the control (Figure 2B). Also, the number of cells exiting the cell cycle (Ki67<sup>+</sup>/BrdU<sup>+</sup> phenotype) markedly increased during the DHA-plus-bFGF treatment (Figure 2C). We did not detect signs of cell death at the time of the cell cycle analysis as assessed by employing the PI and DAPI double-staining method (29) (data not shown).

### 3.3. Expression of immature neural markers

The expression of neural stem/progenitor cell or

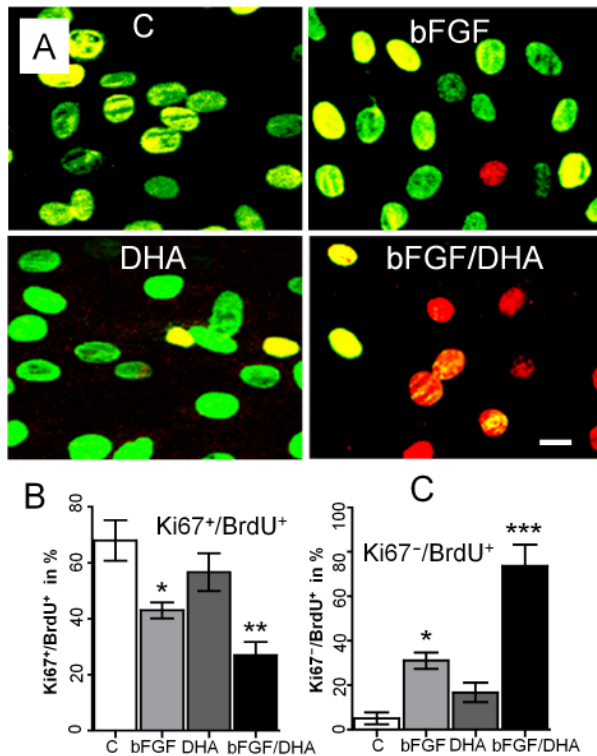


**Figure 2. Cell cycle analysis of BMSC.** (A) Double immunofluorescent staining for Ki67 in green channel and BrdU in red, 72 h after the treatment with the following protocols: C, control group (neurobasal media with N2 supplement); bFGF, treatment with basic fibroblast growth factor; DHA, treatment with docosahexaenoic acid; bFGF/DHA, combination treatment. Scale bar = 20  $\mu$ m. The data, 72 h after the onset of the experiment revealed changes in the proliferation rate being most prominent in the bFGF/DHA-treated group. (B and C) Quantification of the immunoreactive BMSC after 72 h as percentage of all DAPI-positive nuclei and ANOVA statistical analysis with Dunnett post hoc test in the examined groups ( $n = 3$ , error bars represents S.E.M.). There was a statistically significant increase of the cells having quiescent non-proliferative phenotype (BrdU<sup>+</sup>/Ki67<sup>-</sup> cells in red) as well as decreased proliferative phenotype (BrdU<sup>+</sup>/Ki67<sup>+</sup> cells in yellow); \*,  $p < 0.05$  vs. control; \*\*,  $p < 0.01$  vs. control; \*\*\*,  $p < 0.001$  vs. control.

immature neuronal markers nestin and  $\beta$  III-tubulin were examined by immunocytochemistry (Figures 3A-3D), RT-PCR (Figure 3E), and Western blot (Figure 3F). Both nestin and  $\beta$  III-tubulin were positive in the control group, although the  $\beta$  III-tubulin expression was considerably lower (Figures 3A, 3E, 3F, and 3G). One week after the bFGF induction, nestin showed down-regulation concomitant with a  $\beta$  III-tubulin increase, at both mRNA and protein levels (Figures 3B, 3E, 3F, and 3G). The immunocytochemical (Figure 3A) and RT-PCR (Figure 3E) analyses were compatible with the Western blot data (Figure 3F). DHA alone could not cause a significant change in the expression of the examined markers (Figures 3C, 3E, 3F, and 3G). However, DHA addition to the bFGF protocol markedly reduced nestin while significantly enhanced  $\beta$  III-tubulin expression (Figures 3D-3G).

### 3.4. Expression of mature neuronal markers

On the second week after the induction, we examined the expression of the mature neuronal markers such as NF-M and Map2. The control group of BMSC that was cultured in conventional media as well as BMSC treated with DHA alone, exhibited weak expression of mature neuronal markers. In contrast, mature neuronal markers were abundant in the groups treated with bFGF alone or with bFGF plus DHA. Notably, although both bFGF-alone and FGF-plus-DHA protocols induced NF-M and Map2 mRNA, the bFGF-alone protocol could not induce a significant Map2 protein expression (Figures 4A-4C). NF-M/Map2 double-positive cells had long processes (Figure 4D, arrow) and their number was significantly higher during combined bFGF-DHA treatment (Figure 4E).

### 3.5. GPR40 receptor expression

The expression level of GPR40 mRNA and protein were analyzed by RT-PCR, immunocytochemistry, and Western blot in non-treated BMSC, cultured in conventional neural media (control group; Figures 5A, 5E, and 5F), as well as in the three defined experimental conditions of bFGF alone (Figures 5B, 5E, and 5F), DHA alone (Figures 5C, 5E, and 5F), and a combination of bFGF and DHA (Figures 5D-5F). The RT-PCR results were compatible with those of Western blot. GPR40 receptor showed low expression in the control group (Figures 5E-5G) with a predominant localization at the cell membrane (Figure 5A). Interestingly, when BMSC were cultured with bFGF, GPR40 transcripts and protein were significantly upregulated (Figures 5E-5G). The immunostaining showed a cytoplasmic/cell membrane pattern (Figure 5B). In contrast, with DHA alone, GPR40 showed a significantly lower expression (Figures 5E-5G) with a scarce distribution in the cytoplasm and negligible immunofluorescent signal at the cell membrane (Figure 5C). There were no significant changes in the GPR40 expression observed when DHA was applied in addition to bFGF, as compared to the control. By the comparison between the bFGF-alone group and bFGF-DHA group, the latter showed a significant decrease in the GPR40 production (Figures 5E-5G). The immunostaining pattern of the cells in the bFGF-DHA group was similar to that observed in the DHA-alone group (Figure 5C).

## 4. Discussion

In the adult CNS regenerative process associated with both non-ischemic (30,31) and post-ischemic conditions (32-34), bFGF is an important *in vivo* signal for the intrinsic turnover of neural stem/progenitor cells. Similarly, *in vitro*, bFGF can induce neuronal phenotype in BM-MSc by binding to a specific bFGF

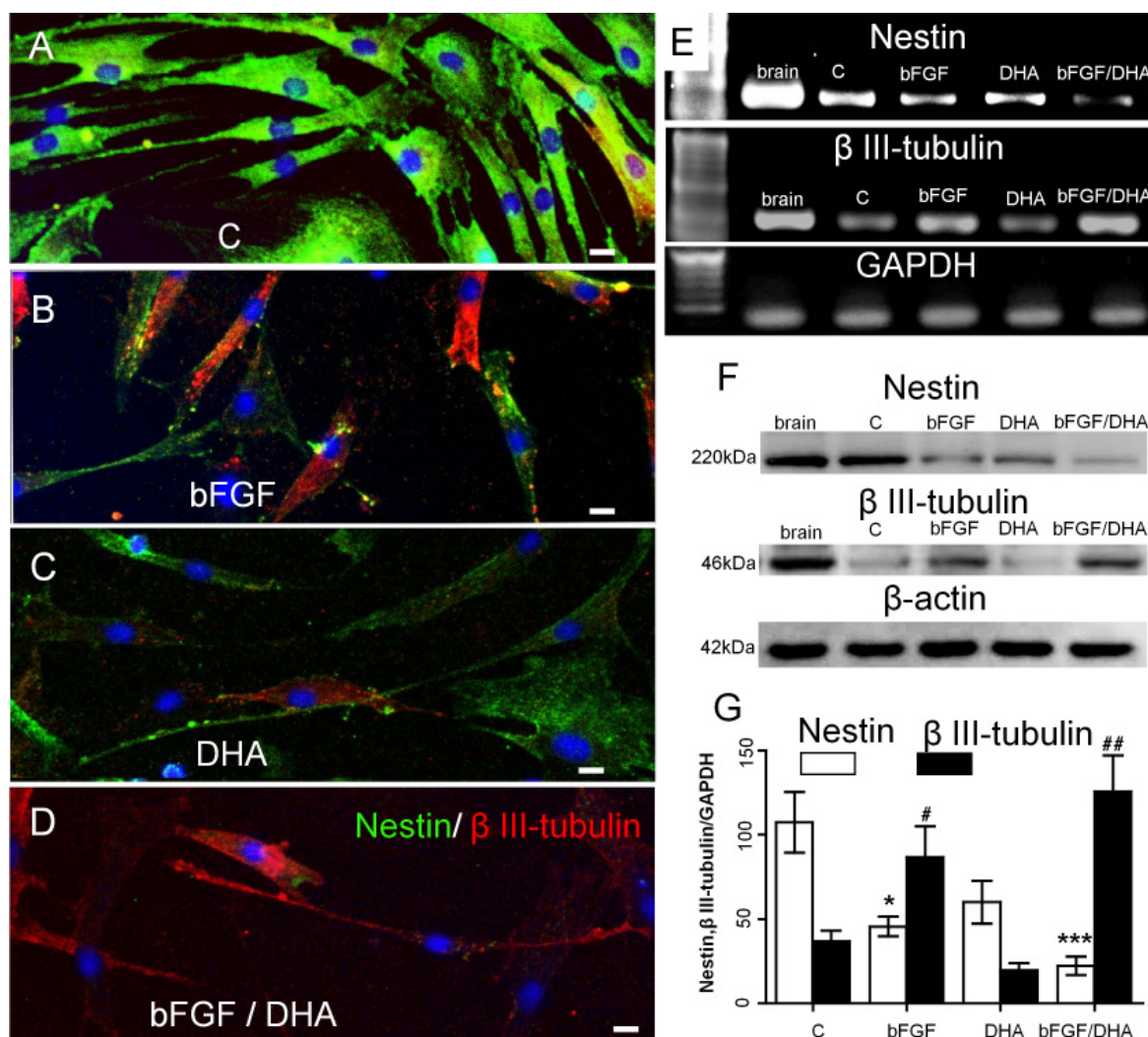


**Figure 3. Expression of neural stem/progenitor marker nestin and immature neuronal marker  $\beta$  III-tubulin 7 days after treatment of clonally-expanded BMSC.** Double immunofluorescent staining for nestin in green and  $\beta$  III-tubulin in red. (A) Control group. (B) bFGF treatment. (C) DHA treatment. (D) bFGF/DHA combination treatment. Scale bars = 20  $\mu$ m. (E) RT-PCR for nestin and  $\beta$  III-tubulin and (F) corresponding immunoblots, showed similar expression level. (G) Quantifications and ANOVA statistical analysis ( $n = 3$ , error bars represents S.E.M.) of the RT-PCR results, nestin and  $\beta$  III-tubulin are calculated as a ratio to GAPDH. \*,  $p < 0.05$  vs. nestin, control; #,  $p < 0.05$  vs.  $\beta$  III-tubulin, control; \*\*\*,  $p < 0.001$  vs. nestin, control; ##,  $p < 0.01$  vs.  $\beta$  III-tubulin, control.

receptor (21). The expression of nestin is widely regarded as a marker for neuronal progenitors. Being gradually replaced by filamentous proteins expressed by functionally mature neurons, nestin shows a temporal relation to the maturation towards neuronal lineage during development. In rodents, although yet controversial, nestin expression is considered also a prerequisite for the specialization of BM-MSC towards the neural lineage (35).

In this study, we confirmed that BMSC express nestin, and bFGF treatment decreases its expression along with the increase in expression of immature neuronal marker  $\beta$  III-tubulin. DHA treatment in addition to bFGF showed that BMSC can express mature neuronal markers such as NF-M and Map2. Interestingly, we found that upregulation of GPR40 receptor is triggered by bFGF. Subsequent DHA addition to the medium, however, provoked the turnover

of GPR40 receptor. The enhancement of neuronal phenotype in BMSC after DHA treatment in addition to bFGF, was consistent with the data from the previous *in vitro* and *in vivo* NSC experiments where an identical relation between stem cell maturation and DHA was found in the course of their neuronal differentiation (10).

Although that BMSC lacked the capacity to produce mature neuronal markers being compared to the control group, when DHA was applied alone (Figure 4), there was a down-regulation of GPR40 receptor expression (Figures 5C, 5E, 5F, and 5G). The observed GPR40 down-regulation can be explained by the concept of 'receptor internalization'. Rapid desensitization and receptor trafficking are well-known to occur for tightly controlling the temporal and spatial regulation of G protein-coupled receptor (GPCR) signaling. In 1996, the  $\beta$ -arrestin-dependent internalization of GPCR that facilitates receptor uncoupling from G proteins, was

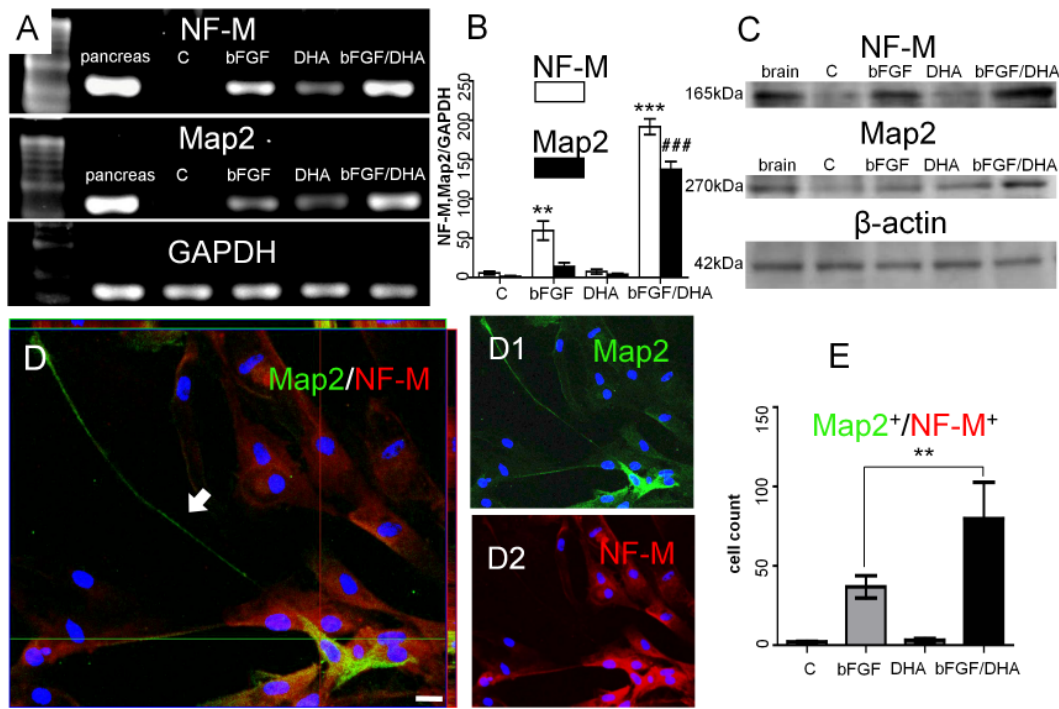


**Figure 4. Expression of mature neuronal markers neurofilament medium chain (NF-M) and microtubule associated protein 2 (Map2) 14 days after treatment of clonally-expanded BMSC.** (A) RT-PCR of NF-M and Map2 and (C) corresponding immunoblots, showed similar expression levels. (B) Quantifications and statistical analysis ( $n = 3$ , error bars represent S.E.M.) of the RT-PCR results subjected to ANOVA. NF-M and Map2 are calculated as ratio to GAPDH. \*\*,  $p < 0.01$ , vs. NF-M, control; \*\*\*,  $p < 0.001$ , vs. NF-M, control; ###,  $p < 0.001$  vs. Map2, control. (D) Double immunofluorescent staining of bFGF/DHA-treated BMSC; NF-M - red, Map2 - green. Scale bar = 20  $\mu$ m. Map2 was positive in the process (D, arrow) and the whole cytoplasm (D1) while NF-M was distributed predominantly in the cytoplasm (D2). Some cells also showed a co-staining in the cytoplasm. (E) The cell number of double-positive NF-M/Map2 was significantly higher in the bFGF/DHA treatment group, compared with the bFGF group (ANOVA, Bonferroni's post-hoc between the two groups bFGF vs. bFGF/DHA; \*\*,  $p < 0.01$ ).

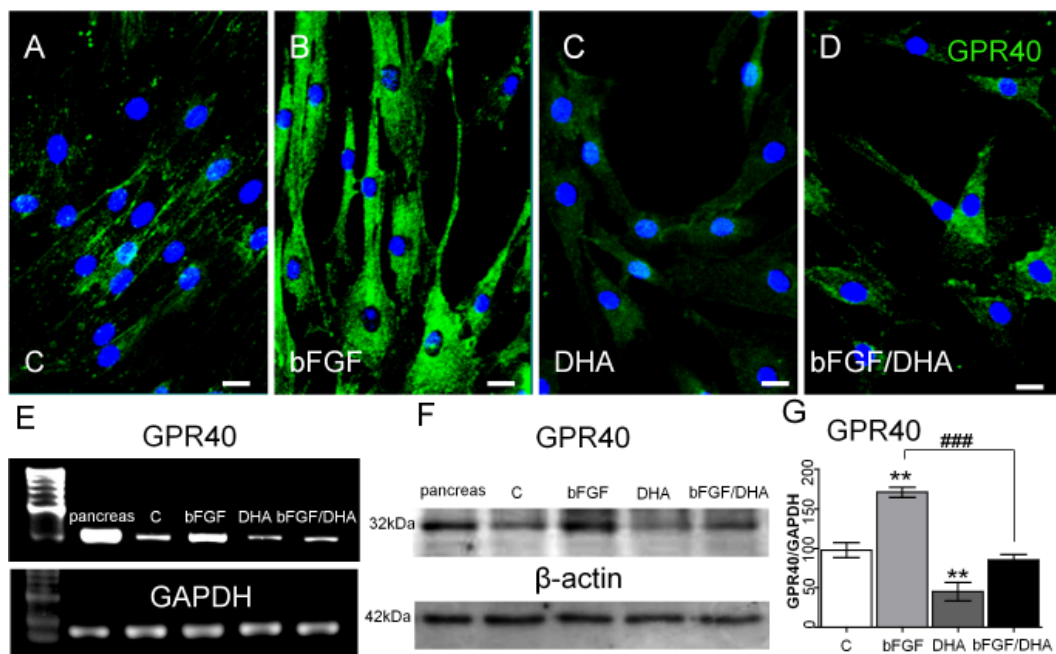


**Figure 5. GPR40 expression.** Immunofluorescent staining of GPR40 in green. (A) Control group, (B) bFGF treatment, (C) DHA treatment, (D) combination bFGF/DHA treatment. Scale bars = 20  $\mu$ m. (E) RT-PCR of GPR40 and (F) immunoblots, showed a similar expression pattern. (G) Quantifications and ANOVA statistical analysis ( $n = 3$ , error bars represents S.E.M.) of the RT-PCR results (\*) and Bonferroni post hoc test (#) comparing DHA versus DHA/bFGF treatments. Values of the GPR40 are calculated as a ratio to GAPDH. \*\*,  $p < 0.01$  vs. GPR40, control; ###,  $p < 0.001$  vs. GPR40 - bFGF, GPR40 - bFGF/DHA. Non-induced BMSC had a low expression of the GPR40 gene distributed at the cellular membranes. bFGF treatment led to a significant increase in GPR40 mRNA, and the protein was abundant in the whole cytoplasm and processes. On the contrary, DHA treatment almost completely abolished the GPR40 gene expression. DHA/bFGF treatment showed no changes in expression profile, being compared to the control group. However, a comparison between the groups with bFGF and DHA/bFGF treatments revealed a significant decrease in GPR40 expression in the last group.

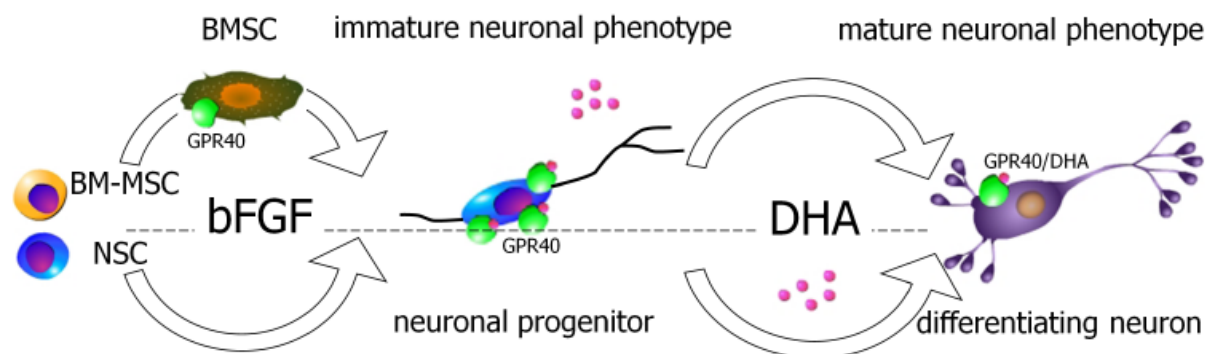


**Figure 6. Hypothetical identities between the DHA/GPR40 signaling in BMSC and NSC.** Bone marrow-derived stromal cells capable of producing neuronal transcripts and proteins - BMSC (over dashed line) are compared to the neural stem/progenitor cells - NSC (below dashed line). The present data indicate that basic fibroblast growth factor - bFGF may have a role in the phenotype induction in BMSC as found in neuronal stem cells, while DHA could be involved in the subsequent steps of transition to mature phenotype. The latter effects might be linked to the expression of the GPR40 receptor by BMSC.

discovered (36-38). After receptor activation,  $\beta$ -arrestins desensitize phosphorylated GPCR, blocking further activation and initiating 'receptor internalization'. GPCR internalization has critical functions to either lysosomal degradative or recycling pathways. Within lysosomes, desensitized GPCR is degraded for the signal termination, whereas in endosomes it is recycled back to the cell surface in a resensitized state (39,40). Although responding to diverse agonists, the structural and functional features of GPCR are remarkably conserved. Since protein kinase C (PKC) is involved in the DHA-mediated signal transduction, the 'receptor internalization' leads to its desensitization, without agonist occupancy of the receptor, dependent only on the PKC activation (39,40). In our experimental paradigm, GPR40, as a specific receptor for DHA, can probably mediate its signaling and contribute to the enhancement of the bFGF-induced upregulation of mature neuronal marker NF-M and Map2, when DHA was applied together.

It remains uncertain whether BM-MSc, which are known to express bFGF receptor (21), can give rise to fully functional neuronal progenitors after bFGF induction *in vitro* (21,23,41). However, bFGF alone is capable of inducing a neuronal phenotype from NSC (42). As summarized in Figure 6, the present data may point out a potential mechanism of DHA-dependent GPR40 signaling in BMSC and its contribution to the enhancement of bFGF-induced expression of neuronal markers. Additional experiments examining the effect of other PUFA on neural stem cells and neuronal progenitors are needed to clarify the role of PUFA/GPR40 signaling in adult neurogenesis (10).

Many features of BMSC remains unclear (16,18), but the discovery of their identity will prospectively define their function and elucidate their biological role (43). In this regard, DHA signaling through GPR40 may have practical implications by providing a strategy for an efficient pre-treatment of BMSC before their

transplantation, since it is now known that BM-MSc expressing neural antigens can instruct a neurogenic cell fate in NSC *in vitro* (44) and potentially *in vivo* (45). Moreover, it is widely accepted that the transplantation of human MSCs and particularly those capable of producing neuronal transcripts and proteins stimulates proliferation, migration, and differentiation of the endogenous neural stem cells (46,47).

#### Acknowledgements

This work was supported by a grant (Creative Scientific Research: 17GS0317, Kiban-Kennkyu (B): 1839039) from the Japanese Ministry of Education, Culture, Sports, Science and Technology.

#### References

1. Briscoe CP, Tadayyon M, Andrews JL, *et al.* The orphan G protein-coupled receptor GPR40 is activated by medium and long chain fatty acids. *J Biol Chem.* 2003; 278:11303-11311.
2. Itoh Y, Kawamata Y, Harada M, *et al.* Free fatty acids regulate insulin secretion from pancreatic beta cells through GPR40. *Nature.* 2003; 422:173-176.
3. Kotarsky K, Nilsson NE, Flodgren E, Owman C, Olde B. A human cell surface receptor activated by free fatty acids and thiazolidinedione drugs. *Biochem Biophys Res Commun.* 2003; 301:406-410.
4. Ma D, Lu L, Boneva NB, Warashina S, Kaplamadzhiev DB, Mori Y, Nakaya MA, Kikuchi M, Tonchev AB, Okano H, Yamashima T. Expression of free fatty acid receptor GPR40 in the neurogenic niche of adult monkey hippocampus. *Hippocampus.* 2008; 18:326-333.
5. Yamashima T. A putative link of PUFA, GPR40 and adult-born hippocampal neurons for memory. *Prog Neurobiol.* 2008; 84:105-115.
6. Ma D, Zhang M, Larsen CP, Xu F, Hua W, Yamashima T, Mao Y, Zhou L. DHA promotes the neuronal differentiation of rat neural stem cells transfected with GPR40 gene. *Brain Res.* 2010; 1330:1-8.
7. Kan I, Melamed E, Offen D, Green P. Docosahexaenoic

- acid and arachidonic acid are fundamental supplements for the induction of neuronal differentiation. *J Lipid Res.* 2007; 48:513-517.
8. Insua MF, Garelli A, Rotstein NP, German OL, Arias A, Politi LE. Cell cycle regulation in retinal progenitors by glia-derived neurotrophic factor and docosahexaenoic acid. *Invest Ophthalmol Vis Sci.* 2003; 44:2235-2244.
  9. Calderon F, Kim HY. Docosahexaenoic acid promotes neurite growth in hippocampal neurons. *J Neurochem.* 2004; 90:979-988.
  10. Kawakita E, Hashimoto M, Shido O. Docosahexaenoic acid promotes neurogenesis *in vitro* and *in vivo*. *Neuroscience.* 2006; 139:991-997.
  11. He C, Qu X, Cui L, Wang J, Kang JX. Improved spatial learning performance of fat-1 mice is associated with enhanced neurogenesis and neuritogenesis by docosahexaenoic acid. *Proc Natl Acad Sci U S A.* 2009; 106:11370-11375.
  12. Cao DH, Xue RH, Xu J, Liu ZL. Effects of docosahexaenoic acid on the survival and neurite outgrowth of rat cortical neurons in primary cultures. *J Nutr Biochem.* 2005; 16:538-546.
  13. Birch EE, Castaneda YS, Wheaton DH, Birch DG, Uauy RD, Hoffman DR. Visual maturation of term infants fed long-chain polyunsaturated fatty acid-supplemented or control formula for 12 mo. *Am J Clin Nutr.* 2005; 81:871-879.
  14. Birch EE, Garfield S, Hoffman DR, Uauy R, Birch DG. A randomized controlled trial of early dietary supply of long-chain polyunsaturated fatty acids and mental development in term infants. *Dev Med Child Neurol.* 2000; 42:174-181.
  15. Fedorova I, Hussein N, Di Martino C, Moriguchi T, Hoshiba J, Majchrzak S, Salem N. An n-3 fatty acid deficient diet affects mouse spatial learning in the Barnes circular maze. *Prostaglandins Leukot Essent Fatty Acids.* 2007; 77:269-277.
  16. Yamashita T, Tonchev AB, Vachkov IH, Popivanova BK, Seki T, Sawamoto K, Okano H. Vascular adventitia generates neuronal progenitors in the monkey hippocampus after ischemia. *Hippocampus.* 2004; 14:861-875.
  17. Kucia M, Zhang YP, Reza R, Wysoczynski M, Machalinski B, Majka M, Ildstad ST, Ratajczak J, Shields CB, Ratajczak MZ. Cells enriched in markers of neural tissue-committed stem cells reside in the bone marrow and are mobilized into the peripheral blood following stroke. *Leukemia.* 2006; 20:18-28.
  18. Meirelles LD, Caplan AI, Nardi NB. In search of the *in vivo* identity of mesenchymal stem cells. *Stem Cells.* 2008; 26:2287-2299.
  19. Hansen A, Chen Y, Inman JM, Phan QN, Qi ZQ, Xiang CC, Palkovits M, Cherman N, Kuznetsov SA, Robey PG, Mezey E, Brownstein MJ. Sensitive and specific method for detecting G protein-coupled receptor mRNAs. *Nat Methods.* 2007; 4:35-37.
  20. Paik MJ, Li WY, Ahn YH, Lee PH, Choi S, Kim KR, Kim YM, Bang OY, Lee G. The free fatty acid metabolome in cerebral ischemia following human mesenchymal stem cell transplantation in rats. *Clin Chim Acta.* 2009; 402:25-30.
  21. Yang HJ, Xia YY, Lu SQ, Soong TW, Feng ZW. Basic fibroblast growth factor-induced neuronal differentiation of mouse bone marrow stromal cells requires FGFR-1, MAPK/ERK, and transcription factor AP-1. *J Biol Chem.* 2008; 283:5287-5295.
  22. Kushida T, Inaba M, Ikebukuro K, Ichioka N, Esumi T, Oyaizu H, Yoshimura T, Nagahama T, Nakamura K, Ito T, Hisha H, Sugiura K, Yasumizu R, Iida H, Ikehara S. Comparison of bone marrow cells harvested from various bones of cynomolgus monkeys at various ages by perfusion or aspiration methods: a preclinical study for human BMT. *Stem Cells.* 2002; 20:155-162.
  23. Kim BJ, Seo JH, Bubien JK, Oh YS. Differentiation of adult bone marrow stem cells into neuroprogenitor cells *in vitro*. *Neuroreport.* 2002; 13:1185-1188.
  24. Jin K, Mao XO, Batteur S, Sun Y, Greenberg DA. Induction of neuronal markers in bone marrow cells: differential effects of growth factors and patterns of intracellular expression. *Exp Neurol.* 2003; 184:78-89.
  25. Jiang YH, Henderson D, Blackstad M, Chen A, Miller RF, Verfaillie CM. Neuroectodermal differentiation from mouse multipotent adult progenitor cells. *Proc Natl Acad Sci U S A.* 2003; 100:11854-11860.
  26. Tao H, Rao R, Ma DD. Cytokine-induced stable neuronal differentiation of human bone marrow mesenchymal stem cells in a serum/feeder cell-free condition. *Dev Growth Differ.* 2005; 47:423-433.
  27. Ma D, Tao B, Warashina S, Kotani S, Lu L, Kaplamadzhiev DB, Mori Y, Tonchev AB, Yamashita T. Expression of free fatty acid receptor GPR40 in the central nervous system of adult monkeys. *Neurosci Res.* 2007; 58:394-401.
  28. Dominici M, Le Blanc K, Mueller I, Slaper-Cortenbach I, Marini F, Krause D, Deans R, Keating A, Prockop D, Horwitz E. Minimal criteria for defining multipotent mesenchymal stromal cells. The International Society for Cellular Therapy position statement. *Cytotherapy.* 2006; 8:315-317.
  29. Lee J, Remold HG, Leong MH, Kornfeld H. Macrophage apoptosis in response to high intracellular burden of *Mycobacterium tuberculosis* is mediated by a novel caspase-independent pathway. *J Immunol.* 2006; 176:4267-4274.
  30. Gritti A, Frolichsthal-Schoeller P, Galli R, Parati EA, Cova L, Pagano SF, Bjornson CR, Vescovi AL. Epidermal and fibroblast growth factors behave as mitogenic regulators for a single multipotent stem cell-like population from the subventricular region of the adult mouse forebrain. *J Neurosci.* 1999; 19:3287-3297.
  31. Pollard SM, Wallbank R, Tomlinson S, Grotewold L, Smith A. Fibroblast growth factor induces a neural stem cell phenotype in foetal forebrain progenitors and during embryonic stem cell differentiation. *Mol Cell Neurosci.* 2008; 38:393-403.
  32. Endoh M, Pulsinelli WA, Wagner JA. Transient global ischemia induces dynamic changes in the expression of bFGF and the FGF receptor. *Brain Res Mol Brain Res.* 1994; 22:76-88.
  33. Lin TN, Te J, Lee M, Sun GY, Hsu CY. Induction of basic fibroblast growth factor (bFGF) expression following focal cerebral ischemia. *Brain Res Mol Brain Res.* 1997; 49:255-265.
  34. Nakatomi H, Kuriu T, Okabe S, Yamamoto S, Hatano O, Kawahara N, Tamura A, Kirino T, Nakafuku M. Regeneration of hippocampal pyramidal neurons after ischemic brain injury by recruitment of endogenous neural progenitors. *Cell.* 2002; 110:429-441.
  35. Wislet-Gendebien S, LePrince P, Moonen G, Rogister B. Regulation of neural markers nestin and GFAP

- expression by cultivated bone marrow stromal cells. *J Cell Sci.* 2003; 116:3295-3302.
36. Freedman NJ, Lefkowitz RJ. Desensitization of G protein-coupled receptors. *Recent Prog Horm Res.* 1996; 51:319-353.
  37. Ferguson SS, Downey WE 3rd, Colapietro AM, Barak LS, Ménard L, Caron MG. Role of beta-arrestin in mediating agonist-promoted G protein-coupled receptor internalization. *Science.* 1996; 271:363-366.
  38. Goodman OB Jr, Krupnick JG, Santini F, Gurevich VV, Penn RB, Gagnon AW, Keen JH, Benovic JL. Beta-arrestin acts as a clathrin adaptor in endocytosis of the beta2-adrenergic receptor. *Nature.* 1996; 383:447-450.
  39. Pierce KL, Lefkowitz RJ. Classical and new roles of beta-arrestins in the regulation of G-protein-coupled receptors. *Nat Rev Neurosci.* 2001; 2:727-733.
  40. Marchese A, Paing MM, Temple BR, Trejo J. G protein-coupled receptor sorting to endosomes and lysosomes. *Annu Rev Pharmacol Toxicol.* 2008; 48:601-629.
  41. Wenisch S, Trinkaus K, Hild A, Hose D, Heiss C, Alt V, Klisch C, Meissl H, Schnettler R. Immunochemical, ultrastructural and electrophysiological investigations of bone-derived stem cells in the course of neuronal differentiation. *Bone.* 2006; 38:911-921.
  42. Roy NS, Wang S, Jiang L, Kang J, Benraiss A, Harrison-Restelli C, Fraser RA, Couldwell WT, Kawaguchi A, Okano H, Nedergaard M, Goldman SA. *In vitro* neurogenesis by progenitor cells isolated from the adult human hippocampus. *Nat Med.* 2000; 6:271-277.
  43. Slack JM. Origin of stem cells in organogenesis. *Science.* 2008; 322:1498-1501.
  44. Croft AP, Przyborski SA. Mesenchymal stem cells expressing neural antigens instruct a neurogenic cell fate on neural stem cells. *Exp Neurol.* 2009; 216:329-341.
  45. Koh SH, Kim KS, Choi MR, Jung KH, Park KS, Chai YG, Roh W, Hwang SJ, Ko HJ, Huh YM, Kim HT, Kim SH. Implantation of human umbilical cord-derived mesenchymal stem cells as a neuroprotective therapy for ischemic stroke in rats. *Brain Res.* 2008; 1229:233-248.
  46. Munoz JR, Stoutenger BR, Robinson AP, Spees JL, Prockop DJ. Human stem/progenitor cells from bone marrow promote neurogenesis of endogenous neural stem cells in the hippocampus of mice. *Proc Natl Acad Sci U S A.* 2005; 102:18171-18176.
  47. Zhao LR, Duan WM, Reyes M, Keene CD, Verfaillie CM, Low WC. Human bone marrow stem cells exhibit neural phenotypes and ameliorate neurological deficits after grafting into the ischemic brain of rats. *Exp Neurol.* 2002; 174:11-20.

(Received April 19, 2010; Revised April 23, 2010; Accepted April 23, 2010)